Effect of bentonite mass per unit area on the desiccation of geosynthetic clay liners under high temperature and low overburden pressure

Bowei Yu & Abbas El-Zein
School of Civil Engineering, The University of Sydney, Australia

R. Kerry Rowe
Department of Civil Engineering, Queen's University, Canada

ABSTRACT: In some applications where geosynthetic clay liners (GCLs) are used in barrier systems, high temperature may build up on the surface of the GCL. This may lead to dehydration and loss of performance which will, in part, depend on the desiccation and water retention properties of the GCL. This paper presents a series of experimental investigations of GCLs performance under high temperature. The behaviour of two Na-bentonite GCLs, with different mass of bentonite per unit area, is investigated. 1-D column desiccation tests, followed by X-Ray imaging, show that under high temperature (78±1ºC), both GCLs experienced high levels of water loss and desiccation. However, the GCL with the larger mass per unit area had a smaller total cracks area. The drying path of the soil water characteristic curve (SWCC) also shows that the GCL with a greater mass per unit area maintained a higher degree of saturation and lower bulk void ratio at higher suctions.

Keywords: geosynthetics, GCLs, column test, cracks, desiccation, SWCC

1. INTRODUCTION

Geosynthetics Clay Liners (GCLs) are often exposed to high temperature at their top surface. This can drive moisture downwards into the cooler subsoils, and may lead to dehydration of the bentonite (Rowe 2005). When the moisture content of the bentonite in a GCL decreases, shrinkage causes the build-up of tensile forces in the clay which may eventually lead to the development of cracks (Southen and Rowe 2004 and 2005; Azad et al. 2011).

Southen and Rowe (2005) indicated that risks of desiccation increase with higher temperature and lower initial water content in GCLs. Similar conclusions were reported by Azad et al. (2011) for double composite liner systems applied in landfills. In some cases, such as those found in brine or solar ponds, as well as applications involving incineration ash or other heat generating waste, GCLs are exposed to much higher temperatures (up to 90ºC) than those typically found in traditional MSW landfills (~35ºC to 45ºC). In addition, in some of these applications, low overburden pressure (e.g., some solar ponds) further increases the risk of desiccation by generating less compressive stresses in the bentonite (Hoor and Rowe 2013) and lower pre-heating water content (Sarabadani and Rayhani 2014). Therefore, it's critical to develop a greater understanding of the dynamics that lead to the desiccation of different kinds of GCLs, particularly under high temperature gradients and low overburden stress.

In this study, the water retention and thermally-driven dehydration of two Na-bentonite GCLs with different mass per unit area (M_A) of bentonite, were studied. The Soil Water Characteristic Curves (SWCC; also known as water retention curves or WRC) were obtained from a vapour equilibrium analyzer (VSA) along the drying path under isothermal conditions at different temperatures. In a series of 1D column tests, GCLs were allowed to hydrate from the subsoil after which temperature was applied. Moisture changes in the subsoil were recorded and GCLs water contents were measured after the hydration and heating stages. X-ray photographs of the two GCLs after heating were compared to assess the effect of mass per unit area on dehydration and desiccation dynamics.

2. MATERIALS AND METHODOLOGY

2.1 *Material properties*

Two types of GCL with powdered Na-bentonite, both supplied by Geofabrics Australia, were examined. Both GCLs, had a needle-punched nonwoven (NW) cover geotextile and a scrim reinforced (woven + nonwoven) carrier geotextile. The difference between the two GCLs was the higher mass per unit area of the bentonite and cover geotextiles (Table 1). Both GCLs have been shown in the past to withstand temperatures typically found in landfill applications, without desiccation, provided they are properly hydrated prior to the application of heat (Azad et al. 2011). However, their tolerance to significantly higher temperatures remains untested. Table 2 shows results of X-ray fluorescence (XRF) tests, conducted to assess the oxide content of Na-bentonite in GCL_A and GCL_B. A hydro-press with cutting rings of 190 mm and 37 mm diameter were used to cut samples for column studies and VSA, respectively. A well graded sand (SW; Table 3) was used as the subsoil in the column study to provide optimized hydration for GCLs before the heating was started.

Table 1 Basic properties for GCLs examined in this study

Generic name	GCL_A	GCL_B
Manufacturers product designation	X-2000	X-3000
Bentonite type	Powdered Na-bentonite	
Bentonite dry mass per unit area (g/m^2) (measured)	4345	4773
	4250	4700
Bentonite dry mass per unit area (g/m^2) (supplier data)		
Cover geotextile mass per unit area (g/m^2)	300	330
Carry geotextile mass per unit area (g/m^2)	410	410
Hydrated water content under 20kPa overburden pressure (%)	183	175

Table 2 Chemical composition of Na-bentonite in GCL_A and GCL_B GCLs from XRF test (PHILIPS PW2400 XRF conducted at the Mark Wainwright Analytical Centre, UNSW, Australia)

Oxides	SiO_2	Al_2O_3	Fe_2O_3	MgO	Na_2O	CaO	TiO_2	K_2O	P_2O_5	SO_3	LOI
Mass contents (%)	69.22	15.28	2.69	2.33	3.12	0.87	0.47	0.65	0.04	0.04	5.62

Table 3 Subsoil sand properties in column experiments

Contents	Values	Test methods
Specific gravity, G_s (-)	2.65	ASTM D854
Saturated hydraulic conductivity, k_s (m/s)	3.0×10^{-4}	ASTM D5856
Controlled porosity, n (-)	0.33	-
Dry density, ρ_d (g/cm^3)	1.78	-
As placed gravimetric water content, w (%)	11	-

2.2 *Experiments*

2.2.1 *Drying path SWCC test at high suction end*

Specimens of 37-mm diameter were adopted to investigate the change in water content in the GCLs on the drying path when exposed to different temperatures. The Vapor Sorption Analyzer (VSA, Decagon Devices, Inc.) maintained samples on a drying or a wetting path until they reached equilibrium at target relative humidity (RH) in a temperature-controlled environment (15°C to 60°C). In this study, 20°C and 60°C were chosen to represent room temperature and high-temperature conditions, respectively. After each specimen reached equilibrium at each RH point, they were quickly taken out for measurement of mass and height (to calculate volumetric water content θ, degree of saturation S_r and bulk void ratio e_B as a check).

2.2.2 *Column desiccation test*

The columns used in this study consisted of a loading frame, two temperature control cells at the bottom and the top, a soil column, and a base (Figure 1). Different parts were connected by flange rings with an o-ring to keep the whole column sealed. Time domain reflectometry (TDR) sensors (No. 1 to No. 4) were installed along the height of the columns with a spacing of 150 mm. In each case, 10 cm thick layers of sand with initial gravimetric water content w of 11% were compacted in the column to $n=0.33$ and $\rho_d=1.78$ g/cm^3 (Table 3) until a 60-cm thick sand column was filled.
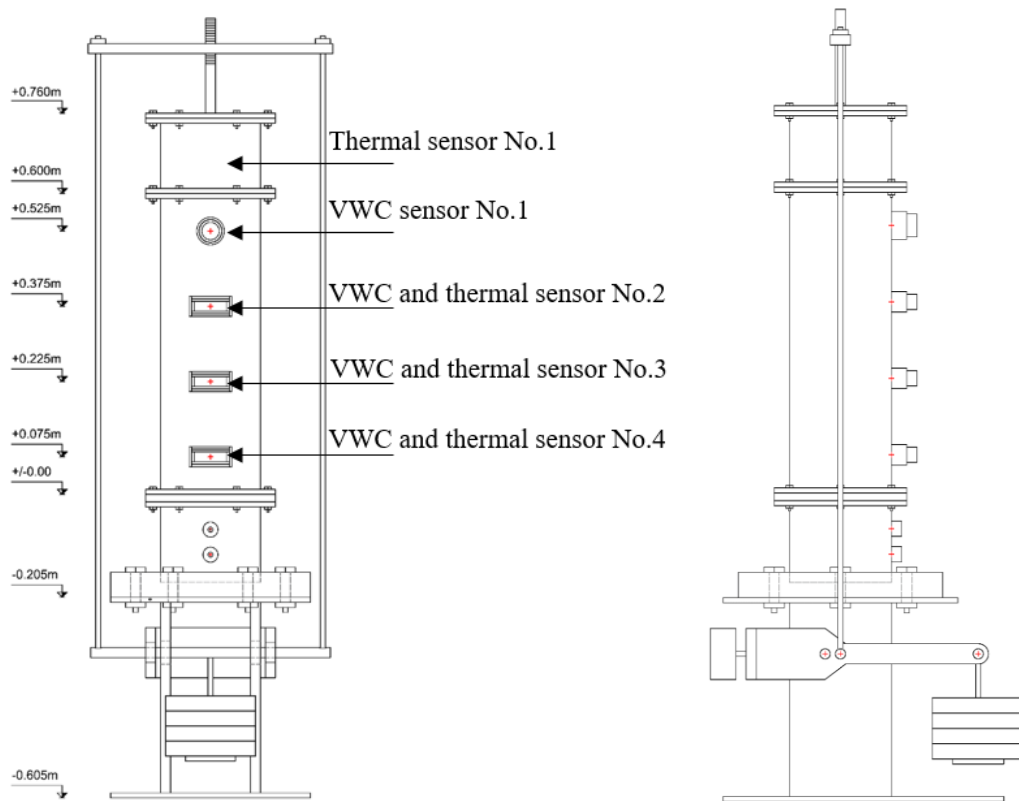
Figure 1. Column diagrams for 1-D desiccation experiment

The column experiments were conducted in three stages: (1) The column was sealed with 20±1ºC applied at both top and bottom and allowed 2-3 weeks for the subsoil to reach moisture equilibrium. (2) A GCL sample was carefully placed on the surface of the sand column, then covered by an HDPE geomembrane (GMB) and allowed to hydrate with moisture from the subsoil, under the same temperature conditions as in stage 1, and 20 kPa overburden load representing a 2 m-deep brine pond (Ghavam-Nasiri et al. 2017). Changes in GCL thickness were monitored for the six to eight weeks required for the GCL to hydrate to an isothermal equilibrium and stop swelling. GCL samples were carefully taken out from the columns and their mass and thickness were measured, after which they were placed back into the columns for the next stage. (3) The temperature at the top was increased to 78±1ºC, while the bottom temperature was kept at 20±1ºC to provide a constant temperature gradient once thermal equilibrium was reached. The overburden load was kept at 20 kPa. Stage 3 was stopped when GCLs height became stable. Each experiment was conducted in two identical columns (namely Column I and II) to assess repeatability.

The temperature and volumetric water content (θ) in the subsoil, as well as change in GCL height were monitored and recorded using TDRs and linear variable displacement transducers (LVDTs) throughout the experiment. At the end of each stage, GCL samples were carefully weighed and their height measured by calipers to confirm the LVDT measurements. The column desiccation testing scheme is summarized in Table 4. At the end of the heating stage, the GCL samples were X-rayed to visualize any desiccation in the bentonite. Finally, the X-ray photos were converted to black and white images using ImageJ to calculate the cracks areas.

Table 4 1-D column desiccation test scheme

Experiment Control Parameters		GCL_A	GCL_B
Duration of Each Stage of Experiment	Subsoil moisture equilibrium	14 days	21 days
	GCL hydration	44 days	56 days
	Heating	39 days	28 days
Temperature applied during equilibrium and hydration stages	Top	20±1ºC	
	Bottom	20±1ºC	
Temperature applied during heating stage	Top	78±1ºC	
	Bottom	20±1ºC	

3. RESULTS AND DISCUSSION

3.1 *Temperature influence on water retention properties of GCLs*

The VSA testing results for GCL_A and GCL_B samples under 20ºC and 60ºC are shown in Figure 2. Ideally, the drying curve should start from the water content that the GCL specimens achieve at the end of the hydration stage in the column ($w \approx 105$ to 140% as shown in Table 5). However, the VSA can only measure suction values higher than 10 MPa, and the purpose here was to evaluate the effect of temperature and mass per unit area on retention at the dry end of the curve, rather than simulate actual field conditions. Therefore, the drying curve as measured by the VSA started from a lower water content. Figure 2 shows that the S_r and w values are small in this range suction. Nevertheless, it can be seen from the 20ºC curves, GCL_B specimens maintain slightly higher S_r values compared to GCL_A (maximum differences of about 4-5% in S_r), although results from the two samples converge at higher suctions (Figure 2a). This is due to the lower bulk void ratio (e_B) of GCL_B compared to GCL_A since gravimetric water contents are similar for the two GCLs (Figure 2b) and e_B is notably lower for GCL_B at all suctions (Figure 3).

For the GCL_B specimen, lower S_r values are found in the lower suction range (30-80 MPa) under 60ºC compared with those under 20ºC, although the differences are small and disappear, once again, at very high suctions. This is consistent with the decrease in surface tension and water retention of bentonite at higher temperatures, widely discussed in the literature (Romero 1999; Villar and Lloret 2004; Tang and Cui 2005; Wan et al. 2015). However, retention in sample GCL_A seems to increase with higher temperature.

(a) Degree of Saturation (S_r) versus total suction

(b) Gravimetric water content (w) variation with total suction
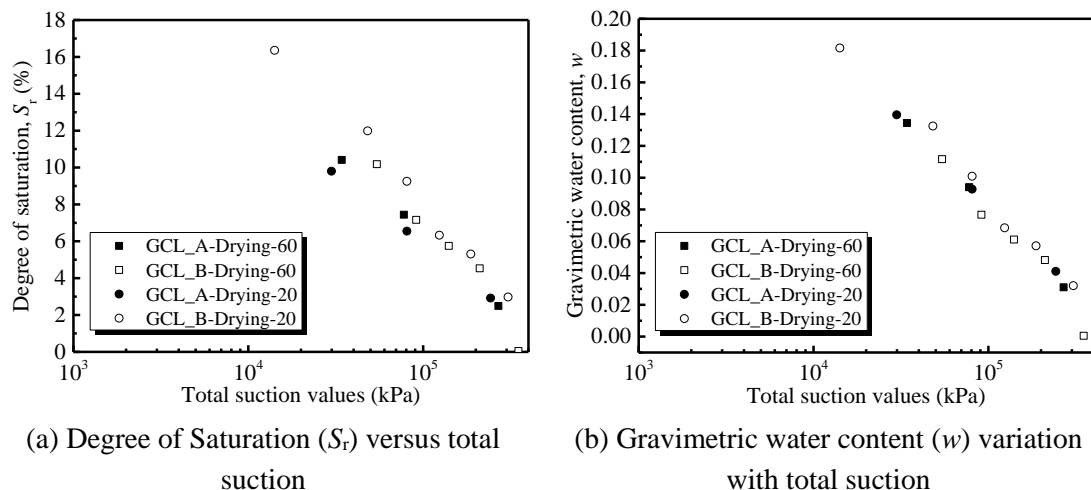
Figure 2. Temperature Effects on SWCC of GCLs

Bulk void ratios (e_B) show a minor decreasing tendency following the drying path for both GCL_A and GCL_B according to Figure 3, which is consistent with results for GCLs at the lower suction end reported by Southen and Rowe (2007). The e_B values of GCL_B specimens are obviously lower than those of GCL_A. An increase in temperature leads to a decrease in the bulk void ratio for GCL_A and but an increase for GCL_B, and no conclusion can be drawn from these results.
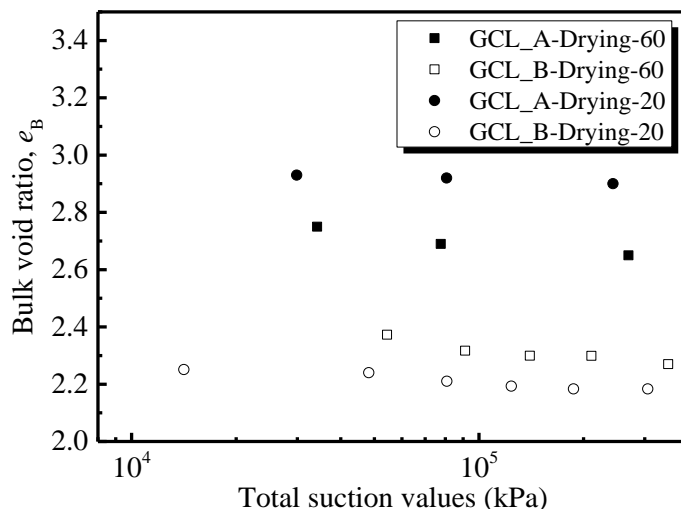
Figure 3. Bulk void ratio variations under drying path

3.2 *Column study results*

3.2.1 *Moisture movement in subsoils*

Variations of θ in the subsoil during the column experiments are shown in Figure 4. Readings from sensor No.3 in GCL_A tests are not presented here because unexpected fluctuations indicated malfunctioning of the sensor (Ghavam-Nasiri et al. 2017). During the hydration stage, TDR sensors 1, 2 and 4 present similar trends for both GCL_A and GCL_B tests. Specifically, TDR No.4 sensors installed at the bottom of the columns, show θ values increasing from an initial ~0.28 to around 0.30-0.32 before the heat was applied. Readings from TDR No.1 and 2 decrease gradually to 0.12~0.15 and 0.15~0.17 respectively. Compared with GCL_A column, moisture readings in the upper part of the subsoil (TDR No.1 and 2) are higher for GCL_B. Meanwhile, TDR No.3 in GCL_B test shows a similar decreasing tendency compared with readings from TDRs No.1 and 2, and stabilizes around 0.18.

After heat is applied on top of the GCLs, readings from sensors 1, 2 and 3 show a sudden rise in water content, in both GCL_A and GCL_B columns, almost certainly due to downward moisture flow caused by GCLs dehydration. This is followed by a gradual decline in moisture content, especially in readings from the top sensor (TDR No.1), due to partial rehydration of GCL by the subsoil driven by suction difference between the two.
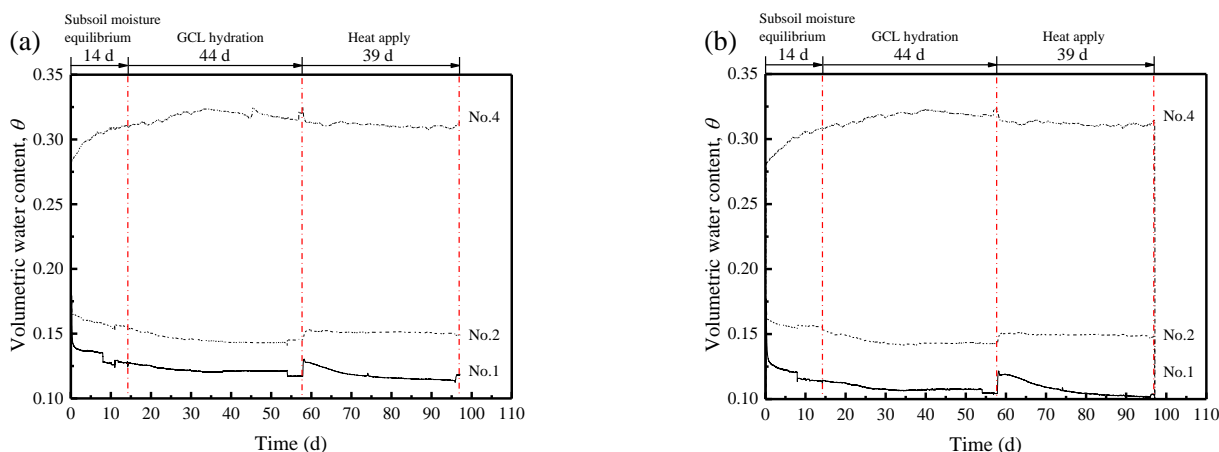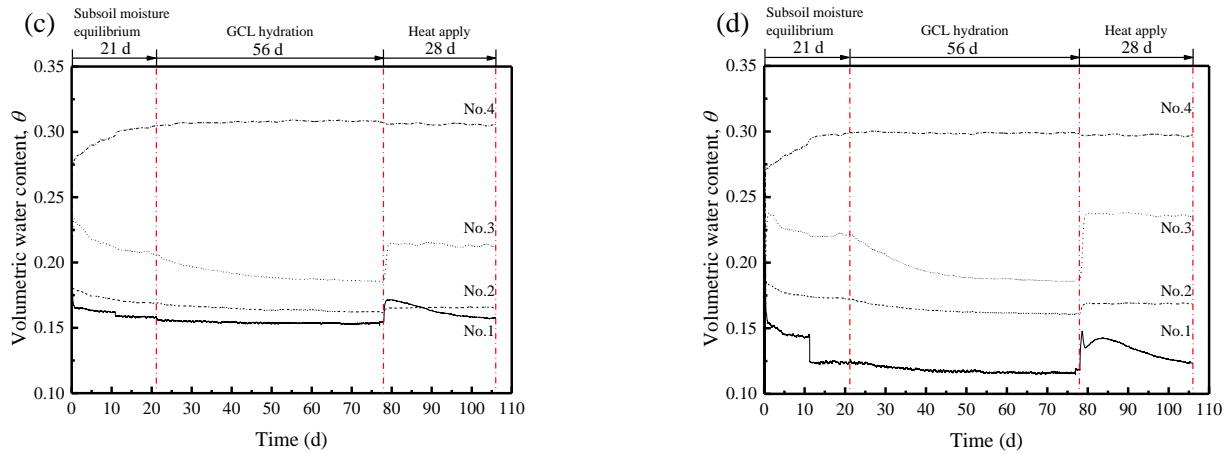
Figure 4. Moisture variations in subsoils during column tests: (a) GCL_A Column I; (b) GCL_A Column II; (c) GCL_B Column I; and (d) GCL_B Column II.

3.2.2 *Effects of hydration and heating on GCL samples*

Table 5 shows height, water content (θ and w), bulk void ratio (e_B) and degree of saturation (S_r) of GCL specimens during the column tests. Bulk void ratios of both GCLs increase during the hydration stage, and decrease after heat is applied, as confirmed by measurements of heights. Compared with GCL_A, GCL_B samples have higher water contents at the end of hydration. This is likely due to longer time given in the experiment for GCL_B hydration (56 days), compared to GCL_A hydration (44 days). Another currently ongoing column study set proves that after 44 days hydration under the same condition, GCL_B samples have w values ranging from 106.0 to 127.5, which are very close to GCL_A w results shown in Table 5. It should be noted that GCL_A samples have smaller e_B values at the end of the heating period compared with GCL_B samples, which is different from results obtained during VSA tests (Figure 3). The 20 kPa loading pressure in the column (not applied in the VSA tests) plays an important role in determining variations in e_B as the samples compressed with the loss of water.

Table 5 GCL sample conditions during the column tests

	Initial condition				End of hydration				End of heating			
	GCL_A		GCL_B		GCL_A		GCL_B		GCL_A		GCL_B	
	I	II	I	II	I	II	I	II	I	II	I	II
Height (mm)*	9.0	8.9	10.5	11.0	10.5	11	12.9	13.8	7.3	7.5	10.0	10.2
Gravimetric water content (w, %)	9.0	9.0	8.9	8.6	105.0	126.0	120.6	140.8	8.4	7.8	8.1	9.2
Volumetric water content (θ, %)	5.0	5.0	6.0	5.3	50.1	56.3	65.5	69.0	5.7	5.1	5.5	6.4
Bulk void ratio (e_B)	2.8	2.8	2.5	2.7	3.4	3.6	3.3	3.6	2.1	2.2	2.3	2.4
Degree of saturation (S_r, %)	4.9	4.9	5.1	4.9	57.4	68.8	68.9	80.5	4.6	4.3	4.6	5.3

*Measured by caliper.

(a) GCL_A Column I   (b)GCL_A Column II

(c) GCL_B Column I   (d) GCL_B Column II
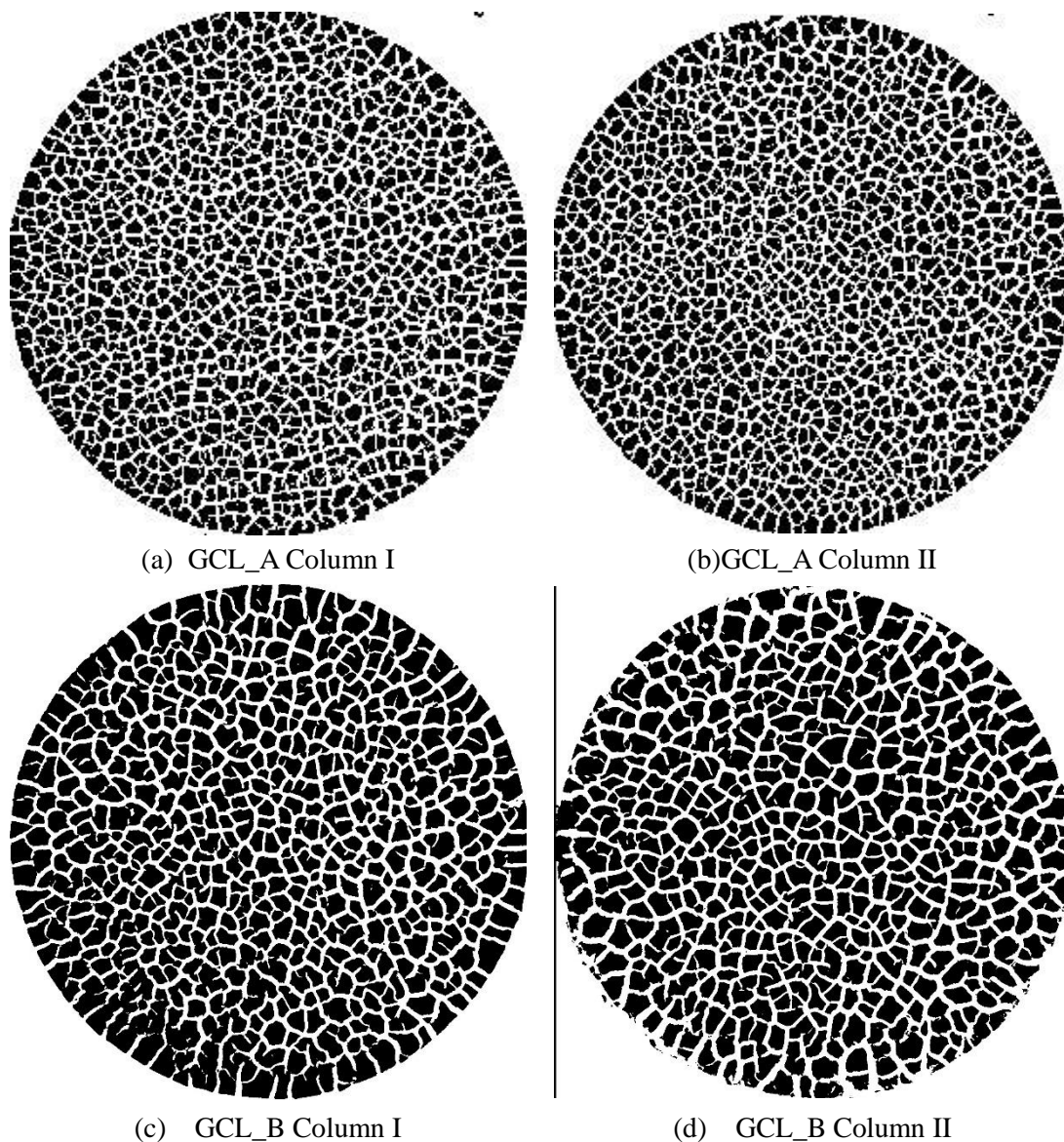
Figure 5. X-ray photographs of desiccated GCL samples from column study

Both GCL_A and GCL_B develop a regular pattern of desiccation cracks over the whole cross section by the end of the heating stage (Figure 5). Compared with GCL_B, GCL_A samples have a larger number of cracks. This is confirmed by calculations of the area of cracks as a proportion of the total cross section, with values of 30.4% to 31.3% for GCL_B and 33.5 to 37.1% for GCL_A. The lower crack density in GCL_B samples compared to GCL_A may be due to their higher water contents prior to heating (120.6% and 140.8% compared to 105.0% found in GCL_A_I) which has been previously shown to reduce risk of desiccation (e.g., Southen and Rowe 2005). Given these differences, it is not possible to attribute the differences in desiccation patterns between GCL_A and GCL_B to differences in M_A. It is worth noting, nevertheless, GCL_A_II and GCL_B_I had similar gravimetric water contents at the end of hydration stage, yet GCL_B_I exhibited a lower percentage, lending some credence to the possible effects of M_A.

4. CONCLUSIONS

Two Na-bentonite GCLs, with different bentonite mass per unit area, were tested for water retention in the high-suction range, and desiccation under heating. The two GCLs were found to have similar water contents at the same suction but GCL_B exhibited higher degrees of saturation because of lower bulk void ratios. The samples were placed in instrumented soil columns, allowed to hydrate from the subsoil, then heated to 78°C, under 20 kPa overburden load. The experiments were conducted in identical pairs to test for repeatability (2xGCL_A + 2xGCL_B). All four samples were found to dehydrate and desiccate when heated. The two GCL_B samples, with higher mass per unit area, were found to have a smaller total desiccated surface area compared to the GCL_A samples, although differences in water content of the samples prior to heating may have contributed to different fissuring patterns.

There is evidence in the literature of a significant capacity of self-healing of bentonite in GCLs and a number of studies have reported that hydraulic conductivity increases due to desiccation may be reversed upon rehydration (Southen and Rowe 2005). It was not possible to measure the hydraulic conductivities of the samples investigated here, in time for inclusion in this paper. However, this is work in progress and hydraulic conductivities of the samples, before and after heating, with deionized water and brine as permeants, will be reported. Based on this, it will be possible to assess the extent to which desiccation leads to increases in hydraulic conductivity and whether differences in desiccation patterns between GCL_A and GCL_B translate into differences in hydraulic conductivity.

ACKNOWLEDGEMENT

REFERENCES

ASTM, D5856. (2015). Standard test method for measurement of hydraulic conductivity of porous material using a rigid-wall, compaction-mold permeameter. *ASTM International*.

ASTM, D854. (2014). Standard test methods for Specific gravity of soil solids by water pycnometer. *ASTM International*.

Azad, F. M., Rowe, R. K., El-Zein, A., & Airey, D. W. (2011). Laboratory investigation of thermally induced desiccation of GCLs in double composite liner systems. *Geotextiles and Geomembranes*, 29(6), 534-543.

Ghavam-Nasiri, A., El-Zein, A., Airey, D., & Rowe, R. K. (2017). Hydration and desiccation of geosynthetic clay liners in composite lining systems under brine pond conditions: A laboratory investigation. In *Proceedings of the 2nd Symposium on Coupled Phenomena in Environmental Geotechnics (CPEG2), Leeds, UK 2017*.

Hoor, A., & Rowe, R. K. (2013). Potential for desiccation of geosynthetic clay liners used in barrier systems. *Journal of Geotechnical and Geoenvironmental Engineering*, *139*(10), 1648-1664.

Romero Morales, E. E. (1999). *Characterisation and thermo-hydro-mechanical behaviour of unsaturated Boom clay: an experimental study*. Universitat Politècnica de Catalunya.

Rowe, R. K. (2005). Long-term performance of contaminant barrier systems. *Geotechnique*, 55(9), 631-678.

Sarabadani, H., & Rayhani, M. T. (2014). Influence of Normal Stress on Hydration of GCLS from Subsoil. *The Journal of Solid Waste Technology and Management*, *39*(4), 292-303.

Southen, J. M., & Rowe, R. K. (2004, January). Investigation of the behavior of geosynthetic clay liners subjected to thermal gradients in basal liner applications. In *Advances in Geosynthetic Clay Liner Technology: 2nd Symposium*. ASTM International.

Southen, J. M., & Rowe, R. K. (2005). Laboratory investigation of geosynthetic clay liner desiccation in a composite liner subjected to thermal gradients. *Journal of Geotechnical and Geoenvironmental Engineering*, *131*(7), 925-935.

Southen, J. M., & Rowe, R. K. (2007). Evaluation of the water retention curve for geosynthetic clay liners. *Geotextiles and Geomembranes*, *25*(1), 2-9.

Tang, A. M., & Cui, Y. J. (2005). Controlling suction by the vapour equilibrium technique at different temperatures and its application in determining the water retention properties of MX80 clay. *Canadian Geotechnical Journal*, *42*(1), 287-296.

Villar, M. V., & Lloret, A. (2004). Influence of temperature on the hydro-mechanical behaviour of a compacted bentonite. *Applied Clay Science*, *26*(1), 337-350.

Wan, M., Ye, W. M., Chen, Y. G., Cui, Y. J., & Wang, J. (2015). Influence of temperature on the water retention properties of compacted GMZ01 bentonite. *Environmental Earth Sciences*, *73*(8), 4053-4061.